Robust helical edge transport in quantum spin Hall quantum wells

Skolasinski, Rafal; Pikulin, Dmitry I.; Alicea, Jason; Wimmer, Michael

DOI
10.1103/PhysRevB.98.201404

Publication date
2018

Document Version
Final published version

Published in
Physical Review B

Rapid Communications

Robust helical edge transport in quantum spin Hall quantum wells

Rafal Skolasinski,[1] Dmitry I. Pikulin,[2] Jason Alicea,[3,4] and Michael Wimmer[1]
[1]*QuTech and Kavli Institute of Nanoscience, Delft University of Technology, 2600 GA Delft, The Netherlands*
[2]*Station Q, Microsoft Research, Santa Barbara, California 93106-6105, USA*
[3]*Department of Physics and Institute for Quantum Information and Matter, California Institute of Technology, Pasadena, California 91125, USA*
[4]*Walter Burke Institute for Theoretical Physics, California Institute of Technology, Pasadena, California 91125, USA*

(Received 14 September 2017; published 14 November 2018)

We show that edge-state transport in semiconductor-based quantum spin Hall systems is unexpectedly robust to magnetic fields. The origin for this robustness lies in an intrinsic suppression of the edge-state g-factor and the fact that the edge-state Dirac point is typically hidden in the valence band. A detailed $\mathbf{k}\cdot\mathbf{p}$ band-structure analysis reveals that both InAs/GaSb and HgTe/CdTe quantum wells exhibit such buried Dirac points for a wide range of well thicknesses. By simulating transport in a disordered system described within an effective model, we demonstrate that edge-state transport remains nearly quantized up to large magnetic fields, consistent with recent experiments.

DOI: 10.1103/PhysRevB.98.201404

Introduction. Topological insulators (TIs) are materials that exhibit a gapped bulk yet enjoy metallic surface or edge states protected by time-reversal symmetry. In particular, two-dimensional (2D) TIs host helical edge modes—i.e., counterpropagating states composed of Kramers partners—that underlie quantized edge conductance [1–3]. Consequently, 2D TIs are often referred to as quantum spin Hall (QSH) systems. The experimentally most studied QSH systems are now based on semiconductor quantum wells. Following the proposal of Bernevig, Hughes, and Zhang [4], the QSH effect was first observed in HgTe/(Hg,Cd)Te quantum wells [5]; various QSH signatures, including quantized edge transport, have by now been identified in this material [6–9].

In HgTe, the QSH effect originates from an inversion of electron and hole bands that is intrinsic to HgTe. This inversion can also be engineered in a multilayer quantum well. In particular, InAs/GaSb quantum wells were also predicted to be QSH systems [10], as they exhibit a so-called broken gap alignment where the conduction band edge of electrons is energetically below the valence band edge of holes. Quantized edge conductance has also been observed in InAs/GaSb [11–13], and the properties of the band inversion and edge-state transport have since been investigated by several experimental groups [14–20].

The hallmark quantized edge conductance in QSH systems originates from time-reversal symmetry, which prevents the helical edge states from elastically backscattering in the presence of nonmagnetic disorder. A magnetic field B breaks time-reversal symmetry, and common expectation dictates that quantized conductance must break down in this case. For example, a magnetic field applied to semiconductor-based QSH systems can directly couple the counterpropagating edge modes, opening up a Zeeman gap in the edge spectrum. It thus came as a surprise that Ref. [13] measured edge conductances that remained quantized with in-plane magnetic fields up to 12 T—sharply defying theoretical expectations.

Here, we show that, contrary to naive expectations, edge-state transport in semiconductor-based QSH systems (HgTe and InAs/GaSb) *typically exhibits a very weak dependence on in-plane magnetic fields.* We have identified three mechanisms for such robustness: (i) The effective edge-state g-factor is strongly suppressed compared to the bulk electron g-factor due to significant heavy-hole contribution in the edge-state wave function. (ii) The Dirac point of the edge states typically resides not in the bulk energy gap, but is hidden in a bulk band. A Zeeman gap opened by the magnetic field appears only at the Dirac point and is thus invisible to transport (see Fig. 1). (iii) Although the combination of disorder and a magnetic field generically permits backscattering, it is strongly suppressed away from the Dirac point due to the nearly antialigned spins of the counterpropagating edge states [see Figs. 1(b) and 1(d)]. This alignment increases for energies away from the Dirac point. When the Dirac point is buried, one then obtains near-perfect quantization of edge conductance in a disordered system out to large magnetic fields of order 10 T as observed experimentally.

We note that buried Dirac points have been predicted and observed in several three-dimensional TIs [21–23]. There are also predictions of buried Dirac points in atomically thin 2D QSH systems [24,25]. Our findings suggest that Dirac-point burial is a common feature also in 2D QSH quantum-well platforms, and has a critical influence on transport in finite magnetic fields.

It was proposed that the edge-state protection in parallel field can also come from finite-momentum exciton condensates [26–28]. Our mechanism is expected to be more robust as it does not require interactions and is stable to disorder.

Suppression of g-factor. We first flesh out the suppression of the edge-state g-factor, which is already accessible from the

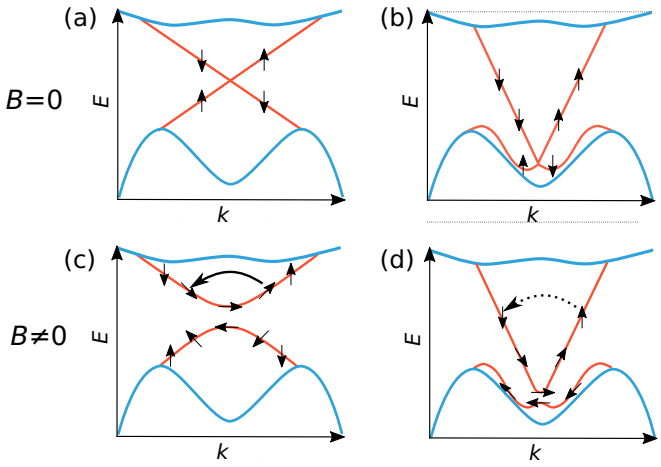

FIG. 1. Schematic depiction of edge-state dispersions: In the absence of a magnetic field, the edge-state crossing is topologically protected, but may (a) reside in the gap or (b) be hidden in a bulk band. In a finite magnetic field, a Zeeman gap opens and the edge-state spins become canted—permitting backscattering as in (c) However, when the edge-state crossing is hidden in a bulk band, spins within the gap are further away from the Zeeman gap and nearly antialign, greatly suppressing backscattering as in (d).

canonical Bernevig-Hughes-Zhang (BHZ) model [4] written as

$$\left[M - B_+\left(k_x^2 - \partial_y^2\right)\right]\psi_1 + A(k_x - \partial_y)\psi_2 = E\psi_1, \quad (1)$$

$$A(k_x + \partial_y)\psi_1 - \left[M - B_-\left(k_x^2 - \partial_y^2\right)\right]\psi_2 = E\psi_2. \quad (2)$$

Here A, M, and $B_\pm = B \pm D$ are BHZ model parameters, x is the propagation direction, y is the direction into the QSH bulk, and $\psi_{1,2}$ respectively denote the electron and hole part of the wave function within one spin sector. The derivation of the effective g-factor is based on computing the wave functions $\psi_{1,2}$ with a hard-wall boundary condition, similar to Ref. [29], and is presented in the Supplemental Material [30]. The result is simple and is based on the relative contributions of electrons and holes in the edge wave functions,

$$g_{\text{eff}} = \frac{g_e B_- + g_h B_+}{B_+ + B_-}. \quad (3)$$

Here, g_e and g_h are electron and hole g-factors, respectively. Equation (3) shows that the effective g-factor of the edge states is the weighted sum of the electron and hole g-factors with their corresponding inverse masses as prefactors.

Typically, g_h is much smaller than g_e; in fact, $g_h = 0$ by symmetry in [001] quantum wells [31]. Moreover, the hole mass usually far exceeds that of electrons, i.e., $B_- \ll B_+$. Together these properties suppress the effective edge-state g-factor considerably compared to bulk values.

We have performed $\mathbf{k}\cdot\mathbf{p}$ simulations (for details see the Supplemental Material [30]) to obtain numerical values for the g-factor in experimentally relevant geometries. For InAs/GaSb we find an edge-state g-factor $g_{\text{eff}} \sim 2$, whereas for HgTe we find $g_{\text{eff}} \sim 8$–10 (in our conventions the Zeeman gap is $g_{\text{eff}}\mu_B B$, with μ_B the Bohr magneton). In contrast,

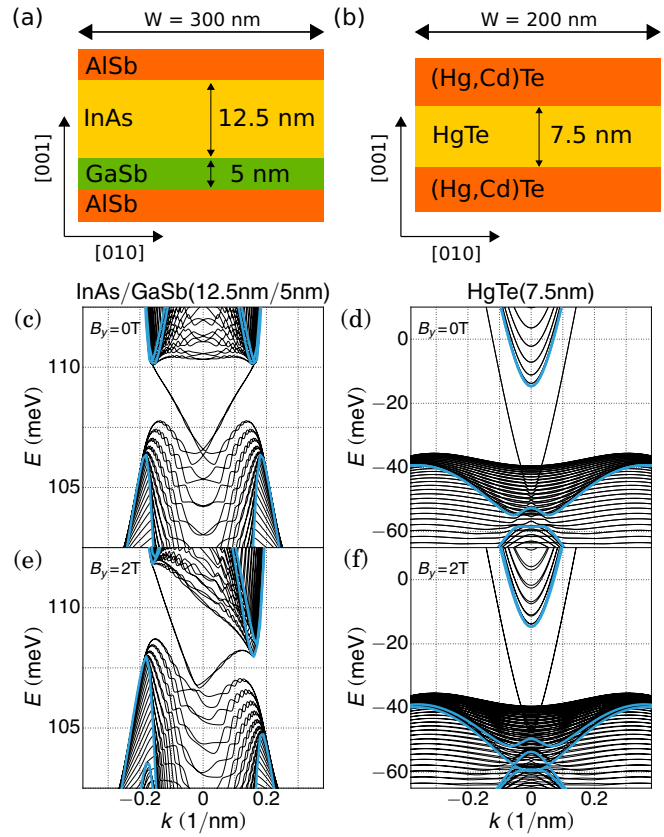

FIG. 2. (a), (b) System geometries used for $\mathbf{k}\cdot\mathbf{p}$ simulations. (c)–(f) Band structures for (c), (e) InAs/GaSb and (d), (f) HgTe/CdTe. For both materials we observe Dirac points buried in a valence band, which obscures the opening of a Zeeman gap under applied in-plane magnetic fields as in (e) and (f).

the bulk electron g-factors are $g \sim 6$–8 in InAs/GaSb and $g \sim 30$–60 in HgTe.

Dirac-point burial from $\mathbf{k}\cdot\mathbf{p}$ *models.* In the "pure" BHZ model given above, the edge-state Dirac point always resides in the gap [29]. Recovering the burial of the Dirac point requires going beyond this minimal model. To this end we now simulate the full semiconductor heterostructure for the experimentally relevant InAs/GaSb and HgTe/CdTe quantum wells. In the numerical analysis we use the 8×8 Kane Hamiltonian [32–34]. Details of the model and material parameters appear in the Supplemental Material [30]. Using a finite-difference method with grid spacing a, we convert the continuous Kane Hamiltonian into a tight-binding model. The resulting energy dispersion are then computed using KWANT [35].

We investigate [001]-grown quantum wells sketched in Figs. 2(a) and 2(b). In particular, we consider InAs/GaSb with AlSb barrier (layer thicknesses 12.5 nm/5 nm as in Ref. [15]), and HgTe with HgCdTe barriers (thickness 7.5 nm as in Refs. [6,9]). Figure 2 shows the dispersion for these heterostructures along the [100] direction. We compare the dispersion for an infinite 2D quantum well without edges (blue lines) to systems of finite width W (black lines) modeled using hard-wall boundary conditions.

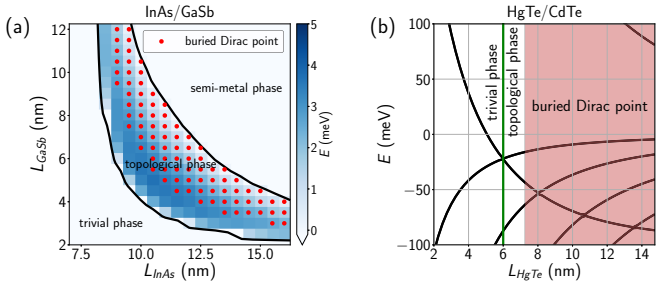

FIG. 3. (a) Topological gap of InAs/GaSb as a function of InAs and GaSb well thicknesses. A red dot indicates a buried Dirac point. (b) Subband edges at the Γ point of HgTe as a function of HgTe well thickness. The Dirac point is buried for thickness $L_{\mathrm{HgTe}} \geqslant 7.25$ nm.

Figures 2(c) and 2(d) respectively illustrate the energy dispersions for InAs/GaSb and HgTe in the absence of a magnetic field. In both quantum wells we observe that the edge-state crossing is shifted out of the topological gap and buried in the valence band. Note that while the crossing itself is topologically protected, its position inside the gap is not.

The $\mathbf{k}\cdot\mathbf{p}$ results diverge from the BHZ model due to the presence of additional hole states that are close in energy to the electron and heavy-hole (HH) bands forming the inverted band structure. For InAs/GaSb, those states lead to a significant deviation of the band structure at the topological gap from the BHZ model, which only contains momentum up to second order. Those states are energetically much further away from the gap than the size of the gap itself [no additional hole states are visible in Fig. 2(c)]; nevertheless, they strongly influence the gap edges at finite momentum, as the coupling between bands increases with momentum [30]. In the case of HgTe a second HH band crosses with the topological gap. Since it only weakly interacts with the edge state, the Dirac point is deeply hidden in this additional band.

Figures 2(e) and 2(f) show the energy dispersions in a finite magnetic field. For both quantum wells, the Zeeman splitting of the edge states remains well hidden in the valence band. Note that while the InAs/GaSb bulk band structure and bulk transport therein is affected by an in-plane field due to orbital effects on the tunneling between the two layers [15,36], this modification neither removes the edge states [37] nor the position of the edge-state crossing [38].

Figure 3 summarizes our simulations for different quantum-well thicknesses: Fig. 3(a) shows the topological phase diagram of InAs/GaSb as a function of layer thicknesses (a nonmonotonic behavior of the topological gap was also previously found in Ref. [39]), while Fig. 3(b) shows the HgTe band edges as a function of layer thickness (here, we only have one parameter). In both cases we indicate when the edge-state Dirac point is buried—which occurs for most of the topological phase space, as expected from our general arguments. The edge-state crossing remains in the gap only close to the topological phase transition; here, only two bands interact in a small range of momentum and can be well described by the BHZ model.

Modeling Dirac-point burial via edge potentials. So far we have considered the edge of the 2D QSH systems simply as a hard wall. However, several semiconducting surfaces additionally exhibit a band bending at the interface. A prominent example is InAs where the band bending can be of the order of 100 meV [40,41]. In fact, band bending has been shown to have significant effects also in InAs/GaSb quantum wells [42,43]. Apart from band bending due to details of the semiconductor surface, gating can also lead to a nonuniform electrostatic potential near the surface, e.g., due to the change of dielectric constant at the semiconductor/vacuum interface.

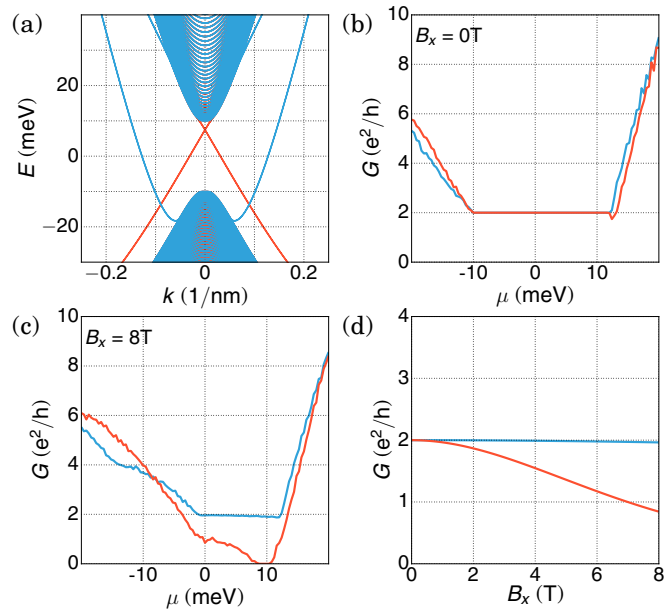

FIG. 4. (a) Band structure and (b)–(d) transport calculations for the BHZ model with (blue) and without (red) an additional edge potential V_{edge}. Transport calculations were performed for a disordered system at (b) zero field and (c) with an in-plane field $B_x = 8$ T. (d) Transport calculation at fixed $\mu = 3$ meV. All transport calculations are averaged over 50 different disorder realizations, with parameters $V_{\mathrm{edge}} = -0.14$ eV, $U_0 = 0.05$ eV, $L = 4000$ nm, $W = 1000$ nm, and finite-difference grid spacing $a = 4$ nm.

A position-dependent potential $V(y)$ that changes only close to the surface (edge potential) has a strong effect on the edge-state dispersion: Within first-order perturbation theory it leads to a shift $\Delta E(k_x) = \langle\psi(k_x)|V|\psi(k_x)\rangle$. In particular, since bulk states are affected little by the edge potential, the edge-state crossing is shifted by $\Delta E(k_x = 0)$ with respect to the bulk bands. Thus, if the edge potential is much larger than the topological gap, it also leads to a burying of the Dirac point. (The edge potential may also give rise to trivial edge states that are also expected to be insensitive to a magnetic field. In contrast to topological edge states these are not expected to be protected from scattering, leading to a length dependence of the edge conductance [42].)

Figure 4(a) shows the burying of the edge-state Dirac point obtained from a finite-width BHZ model supplemented by an edge potential. We use the BHZ parameters for HgTe of Ref. [44] and a finite-difference tight-binding model, with an extra potential V_{edge} at the outermost lattice point. For $V_{\mathrm{edge}} = 0$ (red lines) we find the usual dispersion with the edge-state crossing in the band gap. A finite $V_{\mathrm{edge}} \neq 0$ (blue lines) leaves the bulk states nearly unchanged, but indeed moves the edge-state crossing into the bulk. In particular,

we chose $V_{\text{edge}} = -0.14$ eV which gives a Dirac point burial similar to what we observed from our $\mathbf{k}\cdot\mathbf{p}$ calculations in Fig. 2(d).

Apart from potentially being physically present in semiconductor devices, we can also use the edge potential purely as a tool that leads to a Dirac-point burial within the BHZ model. This is particularly advantageous for numerical calculations, which are far more costly for a 3D $\mathbf{k}\cdot\mathbf{p}$ model.

Quantized conductance in strong in-plane magnetic fields. So far we have emphasized generic mechanisms for hiding the edge-state Zeeman gap within a bulk band. In such cases, observing a clear field-induced edge-state gap through transport would certainly be challenging. Yet, time-reversal symmetry is broken by an in-plane magnetic field, and backscattering from disorder is allowed also *outside* the edge-state Zeeman gap. Naively, a magnetic field should thus lead to an appreciable breakdown of the conductance quantization.

We will now argue that, in practice, conductance may stay nearly quantized even in very strong magnetic fields ($B \gtrsim 10$ T): From Fermi's golden rule we find that the mean free path of edge states in a disordered potential is given as [26]

$$l_{\text{tr}} = \frac{c\hbar^2 v_{\text{F}}}{V_{\text{dis}}^2 \xi}\left(\frac{\delta\mu}{g_{\text{eff}} B}\right)^2. \tag{4}$$

Here, v_{F} is the edge-state velocity, c is a numerical factor ~ 1, $\delta\mu$ is the energy with respect to the edge-state crossing, and we assumed uncorrelated disorder $\langle V(x)V(x')\rangle = V_{\text{dis}}^2 \xi \delta(x - x')$. In the bulk-insulating regime, burial of the edge-state crossing implies that $\delta\mu$ must be of order or larger than the gap size. Together with the strong suppression of the edge-state g-factor g_{eff} discussed earlier, $(\delta\mu/g_{\text{eff}}B)^2$ then is a large factor. Physically, this suppression of backscattering away from Dirac point originates from the fact that kinetic energy efficiently antialigns spins of the edge state away from the Zeeman gap even in the presence of magnetic field; recall Fig. 1(d). In practice, the suppression of scattering presented here may rival that arising from bona fide topological protection at zero magnetic field.

To further quantify the suppression of backscattering, we have performed conductance calculations for a disordered BHZ model, with and without an edge potential, i.e., with and without burying of the Dirac point. As for the results sketched in Fig. 4(a), we use the HgTe parameters from Ref. [44], and compute transport through a rectangular region of length L and width W. We use a random disorder potential drawn independently for every lattice point from the uniform distribution $[-U_0/2, U_0/2]$, and compute the conductance using KWANT [35]. At zero magnetic field [Fig. 4(b)] both models show almost identical transport properties. In particular, the conductance in the gap is perfectly quantized due to topological protection. This behavior changes drastically once a strong in-plane magnetic field is applied [Fig. 4(c)]: Without an edge potential, the conductance drops well below the quantized value of $2e^2/h$. Disorder leads to backscattering within the complete range of energies in the topological gap (not only the small Zeeman gap opened in the edge-state spectrum). When the edge-state crossing is buried, by contrast, conductance inside the gap stays almost perfectly quantized. This stark contrast can also be seen in Fig. 4(d) where we plot conductance as a function of magnetic field for a fixed chemical potential residing in the bulk gap.

Conclusions. In contrast to common expectation, we have shown that the edge-state conductance quantization in semiconductor QSH systems can be surprisingly robust against in-plane magnetic fields. This may be a possible explanation for the surprising findings of Ref. [13], and we could expect to find similar robustness in HgTe. Our findings also highlight a challenge for proposals to use QSH edges as a Majorana platform [45,46]: Localizing Majorana zero modes requires the ability to align the chemical potential within the edge-state Zeeman gap, which could require exceedingly large fields if the Dirac point is buried in a bulk band. A good strategy to overcome this obstacle is to operate in a regime closer to the topological phase transition where the edge-state crossing remains in the gap (if edge potentials are unimportant). Alternative, a side gate might be used to apply an electrostatic potential to move the Dirac point back in the topological gap. These strategies may also allow one to finally observe a strong in-plane magnetic field dependence that would distinguish topological from trivial edge states—the latter naturally exhibiting little field dependence.

Note added. Recently, we became aware of a related work [47] that found a hidden Dirac point in the band structure of InAs/GaSb within an effective six-band model, in qualitative agreement with our full $\mathbf{k}\cdot\mathbf{p}$ calculations.

Acknowledgments. We acknowledge useful discussions with L. Molenkamp, A. R. Akhmerov, and T. Hyart. R.S. and M.W. were supported by the Dutch national science organization NWO. D.I.P. acknowledges support by Microsoft Corporation Station Q. J.A. gratefully acknowledges support from the National Science Foundation through Grant No. DMR-1723367; the Army Research Office under Grant Award No. W911NF-17-1-0323; the Caltech Institute for Quantum Information and Matter, an NSF Physics Frontiers Center with support of the Gordon and Betty Moore Foundation through Grant No. GBMF1250; and the Walter Burke Institute for Theoretical Physics at Caltech.

[1] C. L. Kane and E. J. Mele, Phys. Rev. Lett. **95**, 226801 (2005).
[2] M. Z. Hasan and C. L. Kane, Rev. Mod. Phys. **82**, 3045 (2010).
[3] X.-L. Qi and S.-C. Zhang, Rev. Mod. Phys. **83**, 1057 (2011).
[4] B. A. Bernevig, T. L. Hughes, and S.-C. Zhang, Science **314**, 1757 (2006).
[5] M. König, S. Wiedmann, C. Brüne, A. Roth, H. Buhmann, L. W. Molenkamp, X.-L. Qi, and S.-C. Zhang, Science **318**, 766 (2007).
[6] A. Roth, C. Brüne, H. Buhmann, L. W. Molenkamp, J. Maciejko, X.-L. Qi, and S.-C. Zhang, Science **325**, 294 (2009).
[7] C. Brüne, A. Roth, H. Buhmann, E. M. Hankiewicz, L. W. Molenkamp, J. Maciejko, X.-L. Qi, and S.-C. Zhang, Nat. Phys. **8**, 485 (2012).
[8] K. C. Nowack, E. M. Spanton, M. Baenninger, M. König, J. R. Kirtley, B. Kalisky, C. Ames, P. Leubner, C. Brüne, H.

Buhmann, L. W. Molenkamp, D. Goldhaber-Gordon, and K. A. Moler, Nat. Mater. **12**, 787 (2013).
[9] S. Hart, H. Ren, T. Wagner, P. Leubner, M. Mühlbauer, C. Brüne, H. Buhmann, L. W. Molenkamp, and A. Yacoby, Nat. Phys. **10**, 638 (2014).
[10] C. Liu, T. L. Hughes, X.-L. Qi, K. Wang, and S.-C. Zhang, Phys. Rev. Lett. **100**, 236601 (2008).
[11] I. Knez, R.-R. Du, and G. Sullivan, Phys. Rev. Lett. **107**, 136603 (2011).
[12] I. Knez, C. T. Rettner, S.-H. Yang, S. S. P. Parkin, L. Du, R.-R. Du, and G. Sullivan, Phys. Rev. Lett. **112**, 026602 (2014).
[13] L. Du, I. Knez, G. Sullivan, and R.-R. Du, Phys. Rev. Lett. **114**, 096802 (2015).
[14] V. S. Pribiag, A. J. A. Beukman, F. Qu, M. C. Cassidy, C. Charpentier, W. Wegscheider, and L. P. Kouwenhoven, Nat. Nanotechnol. **10**, 593 (2015).
[15] F. Qu, A. J. A. Beukman, S. Nadj-Perge, M. Wimmer, B.-M. Nguyen, W. Yi, J. Thorp, M. Sokolich, A. A. Kiselev, M. J. Manfra, C. M. Marcus, and L. P. Kouwenhoven, Phys. Rev. Lett. **115**, 036803 (2015).
[16] S. Mueller, A. N. Pal, M. Karalic, T. Tschirky, C. Charpentier, W. Wegscheider, K. Ensslin, and T. Ihn, Phys. Rev. B **92**, 081303 (2015).
[17] F. Couëdo, H. Irie, K. Suzuki, K. Onomitsu, and K. Muraki, Phys. Rev. B **94**, 035301 (2016).
[18] M. Karalic, S. Mueller, C. Mittag, K. Pakrouski, Q. S. Wu, A. A. Soluyanov, M. Troyer, T. Tschirky, W. Wegscheider, K. Ensslin, and T. Ihn, Phys. Rev. B **94**, 241402(R) (2016).
[19] L. Du, T. Li, W. Lou, X. Wu, X. Liu, Z. Han, C. Zhang, G. Sullivan, A. Ikhlassi, K. Chang, and R.-R. Du, Phys. Rev. Lett. **119**, 056803 (2017).
[20] L. Tiemann, S. Mueller, Q.-S. Wu, T. Tschirky, K. Ensslin, W. Wegscheider, M. Troyer, A. A. Soluyanov, and T. Ihn, Phys. Rev. B **95**, 115108 (2017).
[21] H. Zhang, C.-X. Liu, X.-L. Qi, X. Dai, Z. Fang, and S.-C. Zhang, Nat. Phys. **5**, 438 (2009).
[22] D. Hsieh, Y. Xia, D. Qian, L. Wray, F. Meier, J. H. Dil, J. Osterwalder, L. Patthey, A. V. Fedorov, H. Lin, A. Bansil, D. Grauer, Y. S. Hor, R. J. Cava, and M. Z. Hasan, Phys. Rev. Lett. **103**, 146401 (2009).
[23] C. Brüne, C. X. Liu, E. G. Novik, E. M. Hankiewicz, H. Buhmann, Y. L. Chen, X. L. Qi, Z. X. Shen, S. C. Zhang, and L. W. Molenkamp, Phys. Rev. Lett. **106**, 126803 (2011).
[24] S. Murakami, Phys. Rev. Lett. **97**, 236805 (2006).
[25] X. Qian, J. Liu, L. Fu, and J. Li, Science **346**, 1344 (2014).
[26] D. I. Pikulin and T. Hyart, Phys. Rev. Lett. **112**, 176403 (2014).
[27] L.-H. Hu, C.-C. Chen, C.-X. Liu, F.-C. Zhang, and Y. Zhou, Phys. Rev. B **96**, 075130 (2017).
[28] L. Du, X. Li, W. Lou, G. Sullivan, K. Chang, J. Kono, and R.-R. Du, Nat. Commun. **8**, 1971 (2017).
[29] B. Zhou, H.-Z. Lu, R.-L. Chu, S.-Q. Shen, and Q. Niu, Phys. Rev. Lett. **101**, 246807 (2008).
[30] See Supplemental Material at http://link.aps.org/supplemental/10.1103/PhysRevB.98.201404 for details on the numerical simulations, a higher-order effective Hamiltonian for InAs/GaSb, and effective g-factors for InAs/Gasb and HgTe quantum wells, which contains Refs. [48–58].
[31] R. Winkler, *Spin-Orbit Coupling Effects in Two-Dimensional Electron and Hole Systems* (Springer, Berlin, 2003).
[32] E. O. Kane, J. Phys. Chem. Solids **1**, 249 (1957).
[33] E. O. Kane, in *Physics of III-V-Compounds*, edited by R. K. Willardson and A. C. Beer (Academic, New York, 1966), Vol. 1, p. 75.
[34] G. Bastard, *Wave Mechanics Applied to Semiconductor Heterostructures* (Wiley, New York, 1988).
[35] C. W. Groth, M. Wimmer, A. R. Akhmerov, and X. Waintal, New J. Phys. **16**, 063065 (2014).
[36] M. J. Yang, C. H. Yang, B. R. Bennett, and B. V. Shanabrook, Phys. Rev. Lett. **78**, 4613 (1997).
[37] L.-H. Hu, D.-H. Xu, F.-C. Zhang, and Y. Zhou, Phys. Rev. B **94**, 085306 (2016).
[38] One can see from Fig. 2(e) that the parallel field generates indirect gapless bulk excitations. These bulk states are, however, expected to be more susceptible to localization compared to the edge states.
[39] L.-H. Hu, C.-X. Liu, D.-H. Xu, F.-C. Zhang, and Y. Zhou, Phys. Rev. B **94**, 045317 (2016).
[40] D. C. Tsui, Phys. Rev. Lett. **24**, 303 (1970).
[41] M. Noguchi, K. Hirakawa, and T. Ikoma, Phys. Rev. Lett. **66**, 2243 (1991).
[42] F. Nichele, H. J. Suominen, M. Kjaergaard, C. M. Marcus, E. Sajadi, J. A. Folk, F. Qu, A. J. A. Beukman, F. K. de Vries, J. van Veen, S. Nadj-Perge, L. P. Kouwenhoven, B.-M. Nguyen, A. A. Kiselev, W. Yi, M. Sokolich, M. J. Manfra, E. M. Spanton, and K. A. Moler, New J. Phys. **18**, 083005 (2016).
[43] S. Mueller, C. Mittag, T. Tschirky, C. Charpentier, W. Wegscheider, K. Ensslin, and T. Ihn, Phys. Rev. B **96**, 075406 (2017).
[44] M. König, H. Buhmann, L. W. Molenkamp, T. Hughes, C.-X. Liu, X.-L. Qi, and S.-C. Zhang, J. Phys. Soc. Jpn. **77**, 031007 (2008).
[45] L. Fu and C. L. Kane, Phys. Rev. B **79**, 161408 (2009).
[46] J. Alicea, Rep. Prog. Phys. **75**, 076501 (2012).
[47] C.-A. Li, S.-B. Zhang, and S.-Q. Shen, Phys. Rev. B **97**, 045420 (2018).
[48] M. G. Burt, J. Phys.: Condens. Matter **4**, 6651 (1992).
[49] B. A. Foreman, Phys. Rev. B **56**, R12748(R) (1997).
[50] E. G. Novik, A. Pfeuffer-Jeschke, T. Jungwirth, V. Latussek, C. R. Becker, G. Landwehr, H. Buhmann, and L. W. Molenkamp, Phys. Rev. B **72**, 035321 (2005).
[51] A. J. Pfeuffer-Jeschke, Transport experiments in two-dimensional systems with strong spin-orbit interaction, Ph.D. thesis, Physikalisches Institut, Universität Würzburg, 2000.
[52] E. Halvorsen, Y. Galperin, and K. A. Chao, Phys. Rev. B **61**, 16743 (2000).
[53] P. Lawaetz, Phys. Rev. B **4**, 3460 (1971).
[54] Simulation codes and data, doi: 10.5281/zenodo.1466972.
[55] P. Löwdin, J. Chem. Phys. **19**, 1396 (1951).
[56] J. M. Luttinger and W. Kohn, Phys. Rev. **97**, 869 (1955).
[57] G. L. Bir, *Symmetry and Strain-Induced Effects in Semiconductors* (Wiley, New York, 1974).
[58] D. G. Rothe, R. W. Reinthaler, C.-X. Liu, L. W. Molenkamp, S.-C. Zhang, and E. M. Hankiewicz, New J. Phys. **12**, 065012 (2010).